Key Engineering Materials
ISSN: 1662-9795, Vol. 926, pp 2050-2059
doi:10.4028/p-w0hue6

Submitted: 2021-12-08
Revised: 2022-02-02
Accepted: 2022-02-03
Online: 2022-07-22

FE Crash Modeling of Aluminum-FRP Hybrid Components Manufactured by a Hybrid Forming Process

Saarvesh Jayakumar[a*], Lorenz Stolz[b], Sharath Anand[c], Amir Hajdarevic[d], Xiangfan Fang[e],

University of Siegen, Institute of automotive lightweight design, Germany

[a]saarvesh.jayakumar@uni-siegen.de, [b]lorenz.stolz@uni-siegen.de,
[c]sharath.anand@uni-siegen.de, [d]amir.hajdarevic@uni-siegen.de, [e]xiangfan.fang@uni-siegen.de

Keywords: crash modeling, hybrid forming, anisotropic

Abstract. Through the patented process of hybrid forming [1], it is possible to produce a bonded metal-plastic-hybrid component in one process step with the help of an edge-sealed pressing tool. Such a component exhibits an enormous energy absorption potential. To use this complete potential, a reliable FE-Modeling is necessary, that can exactly replicate the complex material layup consisting of an isotropic metal, a very thin bonding layer, and an anisotropic glass mat reinforced thermoplastic (GMT) for crash load case. A methodology is proposed to numerically predict the behavior of the GMT -aluminum hybrid components. And finally, the FE-model could be validated by the experimental results both on three-point bending and axial crash tests on hybrid components.

1. Introduction

Due to their high specific strength and specific energy absorption capabilities, fiber-reinforced thermoplastics (FRP) have proven their potential and are increasingly being used for lightweight design in many structural applications especially in the automotive sector [2,3]. Today, many approaches exist to incorporate FRPs into Body-in-White components and energy-absorbing structures [1].

However, pure FRP components show some disadvantages, such as high production costs [4]. Hybrid metal-FRP components can compensate for these shortcomings by the combination of the beneficial ductile failure behavior of metals with high specific stiffness and strength of the FRP.

According to [4,5], hybrid FRP-metal square tubes produced increased energy absorption. When compared to the pure FRP components, integrating FRP with the metallic structures offers further additional benefits such as cost savings and exceptional structural stability, which justifies their use in automotive applications.

Conventional hybrid forming of FRP-metal components requires multiple stages, which increases the processing time. In order to reduce the processing time, a colossal single-stage hybrid forming process is introduced. A schematic sketch of the hybrid forming process is illustrated in Fig. 1. The fiber-reinforced thermoplastic used in the hybrid forming process corresponds to a glass mat thermoplastic material (GMT). In this process, the mold consists of a die, a punch, and a blank holder. The metal sheet used for the hybrid forming process is pre-coated with the bonding agent. Firstly, an extrudate based on Polypropylene – GMT is heated by an infrared radiator to a semi-molten state and further transferred to the mold along with the pre-coated metal sheet which is closed by a hydraulic press [1].

When the mold closes, the internal pressure in the semi-molten GMT rises, and the metal sheet gets formed simultaneously with the GMT, producing hybrid components [1].

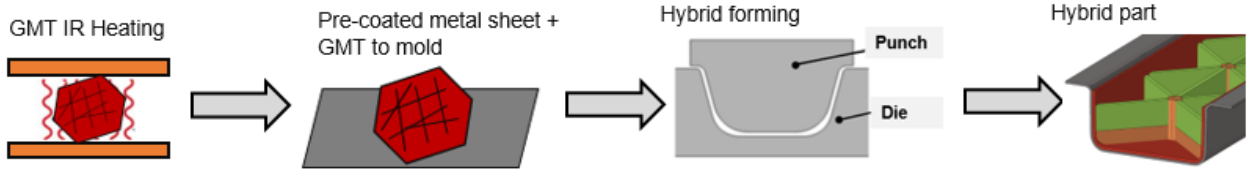

Fig. 1: Schematic sketch of the novel hybrid pressing process [1]

GMT material used in the hybrid forming process has a complex architecture comprising of both continuous fibers (glass mat fibers including two layers of stacked woven fabric reinforcement in a single ply) and discontinuous fibers (long glass fibers) combined with Polypropylene resin.

Since GMT components exhibit anisotropic behavior and more sophisticated energy dissipation mechanisms, material modeling of these materials requires a thorough understanding of their properties [4]. Similarly, failure modeling of adhesives (interlaminar failure) is also crucial because the Metal - GMT material combination leads to complex mutual interactions of aluminum and GMT during axial crushing.

Hence this work aims to investigate the material behavior of Aluminum, GMT, and adhesive and further to develop a methodology to model the hybrid structures through finite element methods. Finally, the developed methodology in FE simulations will be compared with the experiments of hybrid components manufactured by the novel single-stage hybrid pressing process.

2. Experimental Investigations

2.1 Base Materials and characterization

To investigate the quasi-static mechanical properties of these glass mat thermoplastic materials a tensile test machine of type Zwick Z100 was used, and the tests were carried out at a speed of 2 mm/min.

The strain was measured with an optical strain measuring system, Aramis.

Diagrammatic representations of specimen location from the extrudate and pressed components are shown in Fig. 2. It was not possible to use the ISO 527 Norm specimen from the pressed component because the Norm specimens were longer in size in comparison to the component length. Therefore, a smaller specimen size of 110 mm length, 10 mm width, and 4mm thickness was used in both extrudate (delivered material) and pressed GMT material to characterize the tensile behavior. Compression tests were carried out on samples according to ASTM D6641 standards.

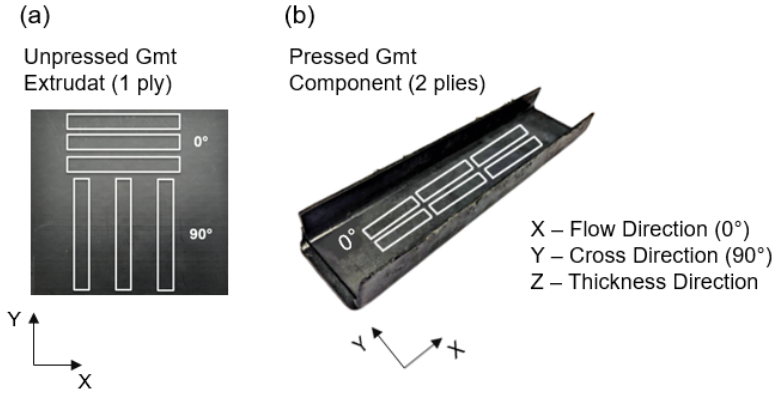

Fig. 2: Specimen location from extrudate (a) and pressed component (b)

After these characterizations were made in the extrudate, the tensile and compression specimens were cut directly from the U profile, which was formed by compression molding using two plies of GMT material. In the pressed GMT, using two plies with two woven layers each increases the number of woven layers to four. Thus, the mechanical properties are expected to be improved in the pressed GMT.

Table 1: Characterized mechanical properties of extrudate (delivered) and pressed GMT materials

Properties		Extrudate	Pressed [2plies]
Young's modulus in longitudinal direction	E_a [GPa]	10.1	11.5
Young's modulus in transversal direction	E_b [GPa]	5.3	7.15
Tensile Strength in longitudinal direction	X_t [MPa]	191	225
Tensile Strength in transversal direction	Y_t [MPa]	89	104
Compressive Strength in longitudinal direction	X_c [MPa]	131	207
Compressive Strength in transversal direction	Y_c [MPa]	85	112

The mechanical properties obtained from the characterization of the extrudate and pressed material are summarized in Table1. We could see a superior behavior in the tensile and compression characteristics for pressed material (2plies) over extrudate. Since these properties directly constitute the component material behaviors these characterization results from the pressed GMT materials are used for the material modeling of GMT in finite element simulations.

The stress-strain behaviors of the base aluminum material 5182 used for the hybrid forming were characterized. For quasi-static tests with lower strain rates, the Zwick Z100 was used, and for high strain rates (from 10 1/s up to 1000 1/s) a high-speed testing machine HTM 5020 was used [6]. Fig. 3a shows the true stress- true plastic strain behavior of aluminum 5182.

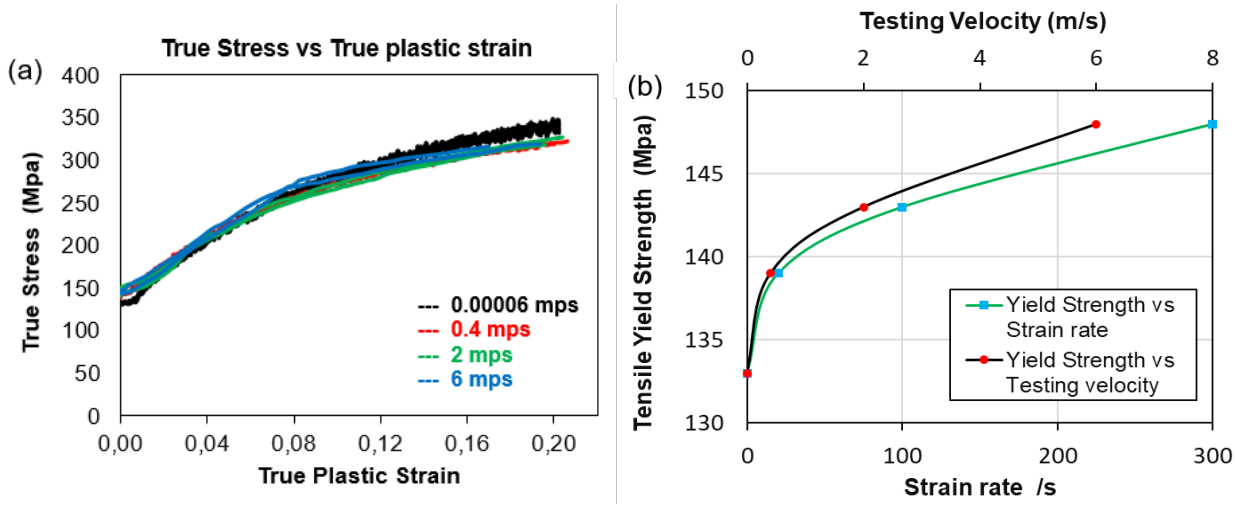

Fig. 3: (a) True Stress-True Plastic Strain behavior of aluminum 5182 at different testing velocities, (b) Tensile yield strength vs loading velocity and Strain rate per second

We could see a very minimal strain rate dependency of aluminum at different loading velocities. High strain-rate deformation of metallic materials involves a significant release of heat to the surroundings, as a result of the so-called thermomechanical coupling effect. By which part of the mechanical work involved in the deformation process is evacuated from the solid as heat. The conversion of thermomechanical work called the Taylor Quinney coefficient varies for different metals at different loading rates [7,8].

The adiabatic heating effect (thermal softening) of the specimens in higher velocities led to a negative influence which produced minimal strain rate dependency of aluminum 5182 materials as shown in Fig. 3. Due to the adiabatic heating effect, very negligible differences in tensile strength values were evidenced between loading velocities 10 mm/min and 30,000 mm/min as shown in Fig. 3b. Similar adiabatic effects were also evidenced in the high-speed testing of metallic materials by P. Larour and T. Emde [7,8].

The determined strain rate dependency from tensile testing was used for the strain rate-dependent material modeling of the aluminum 5182 in dynamic axial crush FE Simulations.

2.2 Lap shear and cross tension tests

To investigate the bonding behavior between Aluminum and GMT in Mode 1 and Mode 2, lap shear and cross tension tests were carried out in the Ibertest Testcom-50 machine. The specimen geometry was based on the DIN EN 1465 standards. The yield stresses 6 MPa and 3.2 MPa were obtained from lap shear and cross tension tests and were further employed to model the interlaminar behavior between hybrid metallic and GMT materials.

2.3 Quasi-Static three-point-bending and dynamic drop tower tests

Two hat profiles manufactured from hybrid forming with different geometrical dimensions for three-point bending and axial crash load cases are shown in Fig. 4. The hat profile geometry of a 3-point-bending load case consists of an X cross rib pattern with cylinders connecting each X cross rib. The hat profile geometry of the axial crash load case consists of an orthogonal rib pattern. The axial crash box component was assembled from two halves of hybrid hat-shaped profiles with self-piercing rivets.

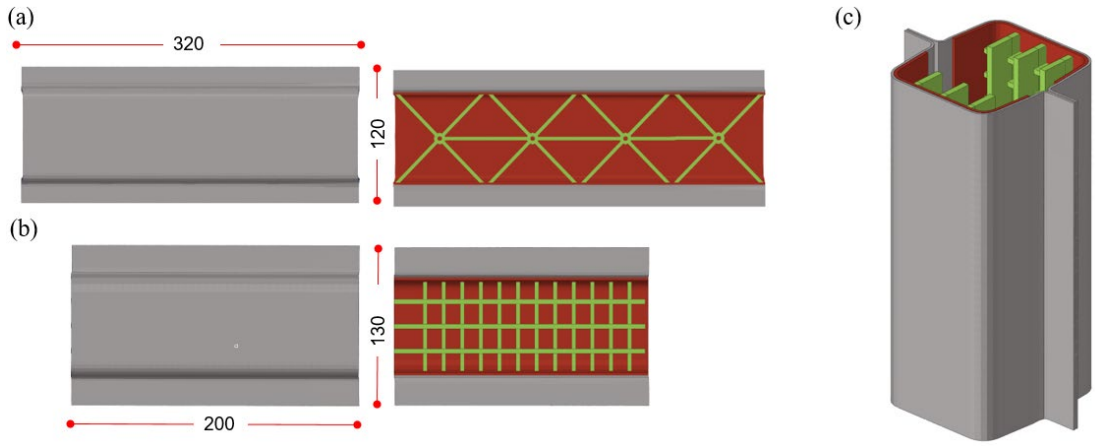

Fig. 4: (a) Hat shaped section for 3-point bending tests, (b) Half hat-shaped section for axial crash tests (c) Assembled two halves of hybrid hat profiles

Quasi-static three-point bending tests were carried out in the Zwick Z100 at a testing velocity of 10 mm /min. The length between the two supports is 200 mm. Bending tests were carried out for specimens with and without closing plates. The testing setup of the Hybrid hat-shaped profile for both three-point bending, and axial crushing is presented in Fig. 5.

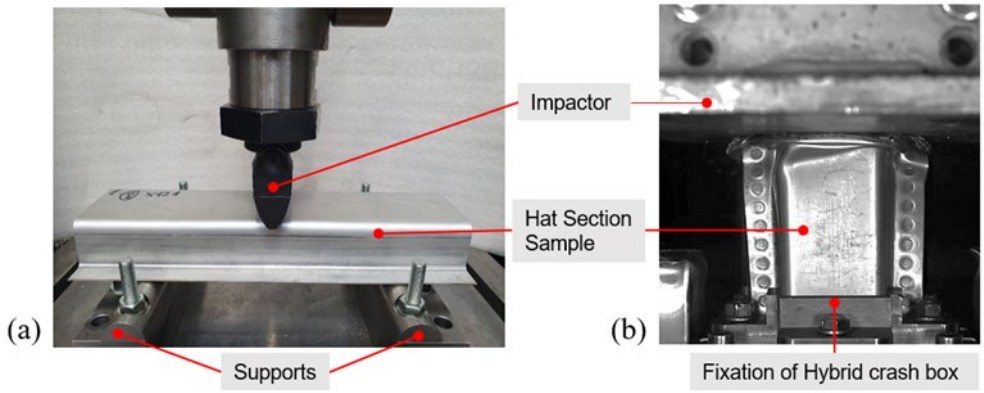

Fig. 5: (a) Quasi-static three-point bending and (b) dynamic drop tower testing of the hybrid profile

Dynamic drop tower tests under axial impact loading of impact velocity 6.2 m/s with a falling mass of 375 Kg yielding kinetic energy of 7KJ were carried out. The bottom portion of the axial crash box is fixed and constrained in all directions up to 50 mm.

3. Finite Element Model

Both the aluminum and GMT in the hybrid hat profile structures were modeled using LS-Dyna as layers using thin shell elements. Thin shells were stacked together and connected by cohesive elements which are shown in Fig. 6. Thin shell elements used for modeling aluminum and GMT are of Type 16 fully integrated shell elements. 8 noded cohesive element of thickness 0.1 mm with four integration points was centered between two layers of shells (Aluminum and GMT) on the lower and upper surfaces to predict the interlaminar behavior. Fig. 6 shows the finite element model of both quasi-static three-point bending and dynamic axial crash load cases. Impactor and supports in both three-point bending and axial crush load cases were modeled as rigid bodies.

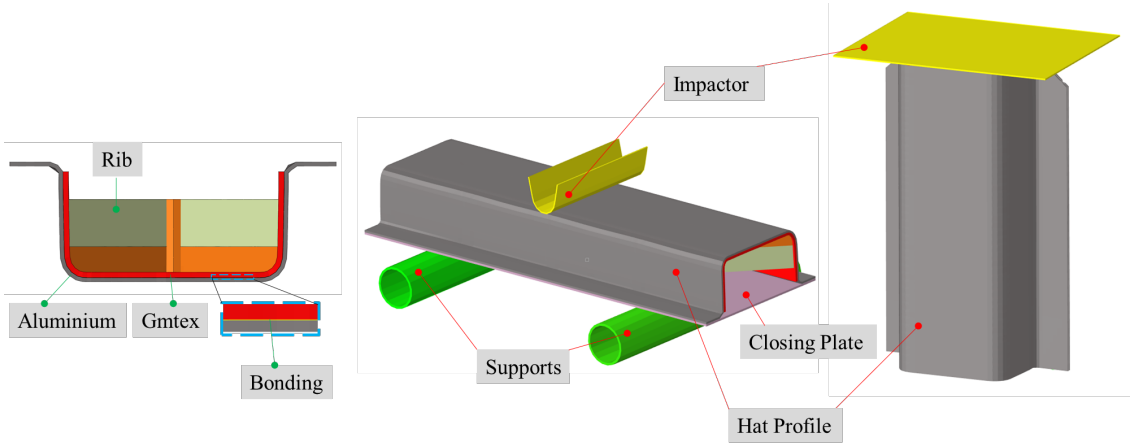

Fig. 6: Hybrid Aluminum – GMT Finite element model

The contact algorithm Contact Automatic Single Surface was used for modeling the contact between impactor, rigid supports, and hybrid hat structures. Further Contact Automatic Surface to Surface was
employed to model the contact between aluminum and GMT layers with a friction coefficient of 0.35.

Since the strain rate effect was negligible (lesser than 5 %) in velocities 30,000mm/min and 10mm/min due to the adiabatic heating effect. The three-point bending load case was simulated under a quasi-static loading with a velocity of 30,000mm/min in comparison to the actual velocity of 10mm/min to minimize the extensive computation time. Additionally, the quasi-static velocity of 30,000mm/min in the simulation was ensured from the energy plots to provide negligible inertial effects in the system.

4. Material Modeling

4.1 Modeling of Hybrid Aluminium – GMT structures

Aluminum 5182 layer in the hybrid structure was modeled using MAT 24 isotropic elastoplastic material model which includes the possibility of different stress-strain curves from the tensile characterization under different velocities which will describe the strain rate dependency of the material.

For modeling the GMT materials an orthotropic material model Mat_Enhanced_Composite_Damage MAT 54 was chosen with an enhanced Chang- Chang failure criterion.

Depending upon the specific degradation law used, the constitutive models in LS-Dyna can be categorized into progressive failure models (MAT 54) and continuum damage mechanics models [9,10].

The progressive failure models are increasingly used for modeling composite materials due to their pragmatic approach and for their ease of design optimizations.

The damage behavior was modeled using the Chang Chang failure criterion with different failure modes in tensile and compression [11,12]. The necessary material parameters X_c, X_t, Y_t, Y_c, E_a, E_b, and further for modeling the GMT materials were obtained from the material characterization of GMT materials summarized in Table 1.

4.2 Interlaminar Failure Modeling of adhesive

In Aluminum GMT Hybrid Structures, the bonding or the interlaminar failure can be modeled by either tiebreak contact or cohesive element [4, 13]. Cohesive zone models can be successfully used to model the fracture behavior of a bonded joint in a crash simulation. In this work, a layer of cohesive elements of 0.1 mm thickness was modeled between Aluminum and GMT layers to simulate the interlaminar behavior.

Fig. 6 shows the models for axial crushing and dynamic three-point bending with multiple layers of shell and cohesive elements. The interlaminar failure between aluminum and GMT material was modeled using *Mat-Cohesive-Mixed-Mode-Elastoplastic-Rate (MAT 240) cohesive material

model. This model includes a tri-linear traction-separation law with a quadratic yield and damage initiation criterion in mixed-mode loading, while the damage evolution is governed by a power-law formulation. The damage initiation and interaction among different delamination modes are described below.

$$\sqrt{\left(\frac{t_s}{s_0}\right)^2 + \left(\frac{t_t}{s_0}\right)^2 + \left(\frac{(t_n)}{t_0}\right)^2} = 1. \quad (1)$$

where the t_0 and s_0 are the critical stresses for Mode I and Mode II/III, respectively [13,14]. These yield stresses were obtained from the Lap Shear and Cross Tension tests: $t_0 = 6$ MPa and $s_0 = 3.2$ MPa. Energy release rate G_{Ic} in mode I and G_{IIc} in mode II was calibrated to two extreme situations in three-point bending load cases which are presented in Fig. 7. The energy release rate G_{Ic} and G_{IIc} obtained from calibrations is 0.8 N/mm.

5. Simulation Results and Analysis

GMT material doesn't flow well in comparison with short fiber-reinforced composite materials, the rib structures were not filled with fiber due to the longer fiber lengths. The characteristics in the profile from the computer tomography scans and microscopy scans were adopted in FE modeling of rib structures. For the three-point bending hybrid profiles, the lower part of the X cross rib was modeled by GMT composite material properties while the upper part was only matrix material.

Microscopical investigations from hybrid crash profiles showed that the horizontal rib filling was very restricted up to only 1mm depth. Therefore, in the modeling horizontal ribs were adopted to have only matrix material properties. The upper part of the longitudinal rib was modeled with matrix properties due to the absence of fibers and the lower part of the longitudinal ribs which had rib filling up to 8.5 mm was modeled as GMT composite material. We could further notice the gradual reduction of fiber volume in rib-filled regions (8.5 mm) of the GMT material in vertical ribs. Similarly, a gradual reduction of fiber volume percentage in the rib filling of GMT material was evidenced by C. Kuhn due to fiber bridging effects [15]. The fiber volume-dependent material properties in the vertical rib-filled region of 8.5 mm in GMT material were not considered in simulations due to the extensive material characterization and intensive microscale finite element modeling.

5.1 Quasi-Static Three-Point Bending

In this analysis, quasi-static three-point bending load cases on the hybrid aluminum – GMT hat profiles were modeled.

To validate the simulative behavior of the adhesives two 3-point-bending tests were compared with experimental investigations under quasi-static loading with and without a closing plate and can be seen in Fig. 7.

It can be seen that the Hat profile with a closing plate shows small bending deflection as the closing plate prevents the opening of the profile and the adhesives are only debonded in the middle section of the hat profile where the impactor is in contact as shown in Fig. 7 (left).

However, when the profile without closing plate was bent, large bending deflection takes place which causes a strong debonding of the aluminum and GMT, as can be seen in Fig. 7 (right). Thus, the simulation model for hybrid structures could qualitatively be validated for both tests.

Fig. 7: Validation of two 3-point-bending load cases with closing plate and without closing plate

5.2 Dynamic Axial Crushing hybrid components

The comparison of experimental and simulation results obtained from dynamic crushing of hybrid profiles is shown in Fig. 8. Further, it can be depicted that including a 45° trigger in the axial crash box for the drop tower tests significantly reduced the initial peak, which was also observed in the finite element simulation results from Fig. 8

From the results in Fig. 8, it can be concluded that the force intrusion behavior of the simulation over-predicts the experimental results till the crushing displacement of 60 mm.

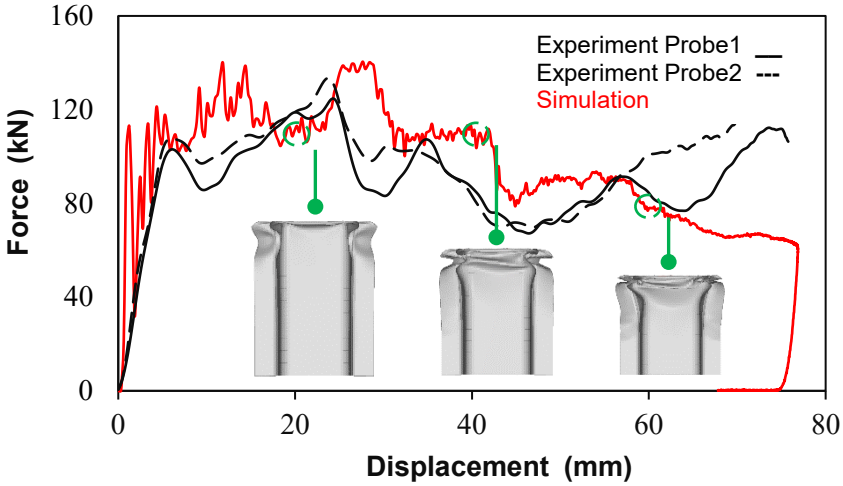

Fig. 8: Correlation of force-intrusion curves in experiment and simulation with 45° trigger

We can depict that the exclusion of the microscale material modeling approach and the assumption of homogeneous fiber volume filling of the axial crash box vertical ribs (up to 8.5mm) could be the reason for the over-prediction of mean force levels in simulations.

On further comparing the mean force level to the experimental behavior we could evidence that the second peak is delayed in the finite element simulations. From Fig. 9 we could see the systematic crushing of the hybrid crash box at different displacement ranges 20mm, 40mm, and 60mm. We can depict the minimal failure of the adhesives in the cut section view at crushing displacement 20 mm. As the crushing proceeds to 60 mm, we can see a predominant failure of adhesives.

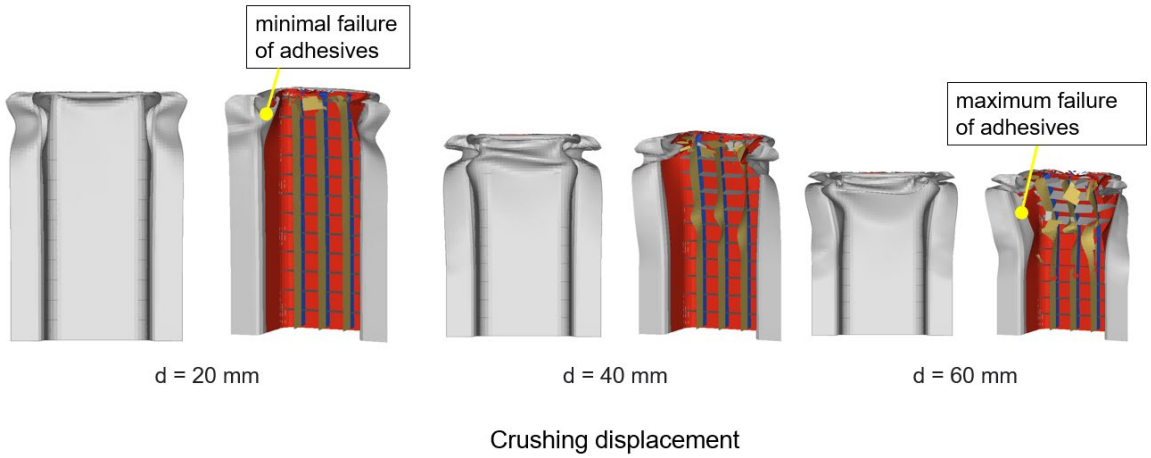

Fig. 9: Crushing behavior of hybrid axial crash box at different displacements

The predominant failure of adhesives after crushing displacement 60 mm causes mutual interaction between aluminum folding and GMT crushing (delamination), leading to an unstable complex failure mechanism. This unstable behavior at the end of the crushing process causes substandard repeatability and a higher discrepancy between the simulation and experiments (Fig. 8 and 9).

The presence of adhesive in the crash box and the corresponding connection strength contributed to a more stable and progressive crushing of the hybrid crash box till the crushing displacement of 60mm.

In Fig. 10 the substantial crushing characteristics of the hybrid crash box's deformation and damage behavior after axial crushing in both experiments and simulation are compared in the top and front view.

The corresponding folds of the axial crash box after crushing are shown. The folds of the aluminum, crushing of GMT and the separation of aluminum and GMT could be modeled successfully which can predict both the crushing characteristics and the crushing parameters such as intrusions and peak force reasonably well.

Fig. 10: Comparison of crushing morphologies from simulation and experiments (Top and front view)

6. Summary and Conclusions

In this study, the material behavior of GMT, aluminum, adhesives materials was determined and implemented into a newly developed FE method. This model combines MAT 24, MAT 54, and MAT 240 of LS-Dyna, and may successfully model the Aluminum-GMT hybrid structures manufactured by the hybrid forming process. A quasi-static three-point bending load case and a dynamic axial crash load case were validated and the following conclusions and inferences were drawn:

- The FE-model developed for the Al-GMT hybrid could reproduce the 3-point-bending tests satisfactorily, and especially capture the failure between the metal and plastic interface in different tests with and without the closing plates in the hat profile.
- Cohesive Zone material model may reproduce the bonding behavior between Aluminum and GMT materials quite exactly.
- The developed material model consisting of the interlaminar failure of the adhesives and intralaminar failure of GMT material could satisfactorily predict the overall experimental crushing behavior of the hybrid crash box.
- The mean force level of the FE simulation over-predicts the experimental behavior until crushing displacement 60mm due to the exclusion of microscale modeling in the fiber-filled regions of the axial crash box.
- A greater disparity was observed between simulation and experiments in the hybrid crash box after a crushing displacement of 60mm, owing to the predominant failure of adhesive, which resulted in complex mutual interactions of aluminum and GMT layers.
- Further, this modeling approach seems to provide a numerically time-efficient and at the same time comprehensive simulation.

Acknowledgments

The authors acknowledge the European regional development funds (EFRE- 0801129) for their financial support of the research project ‘‘AKTIV’’.

References

[1] X.F. Fang, T. Kloska, Hybrid forming of sheet metals with long Fiber thermoplastics by a combined deep drawing and compression molding process, Int. J. of Material Forming. 13 (2019) pp. 561-575.

[2] B. Ahmad, X.F. Fang, Modeling Shear Behavior of Woven Fabric Thermoplastic Composites for Crash Simulations, Applied Composite Materials. 27 (2020) pp. 739-765.

[3] J. Striewe, C. Reuter, Manufacturing, and crashworthiness of fabric-reinforced thermoplastic composites, Thin-Walled Structures. 123 (2018) pp. 501-508.

[4] M.R. Bambach, Axial capacity and crushing of thin-walled metal, fiber-epoxy and compo-site metal-fiber tubes, Thin-Walled Structures. 48 (2010) pp. 440–452.

[5] C. Reuter, T. Tröster, Crashworthiness and numerical simulation of hybrid aluminum-CFRP tubes under axial impact, Thin-Walled Structures. 117 (2017) pp. 1-9.

[6] X.F. Fang, A one-dimensional stress wave model for analytical design and optimization of oscillation-free force measurement in high-speed tensile test specimens. 149 (2021) pp. 103770.

[7] P. Feraboli, B. Wade, LS-Dyna Mat 54 modeling of the axial crushing of a composite tape sinusoidal specimen, Composites: Part A. 42 (2011) pp. 1809-1825.

[8] S. Boria, A. Scattina, Axial energy absorption of CFRP truncated cones, Composite Structures. 130 (2015) pp. 18-28.

[9] F. Chang, K. Chang, Post-failure analysis of bolted composite joints in tension or shear-out mode failure, Journal of Composite Materials. 21 (1987) pp. 809-833.

[10] F. Chang, K. Chang, A Progressive damage model for laminated compositescontaining stress concentrations, Journal of Composite Materials. 21 (1987) pp. 834-855.

[11] G. Zhou, Q. Sun, Crushing Behaviors of Unidirectional Carbon Fiber Reinforced Plastic Composites under Dynamic Bending and Axial Crushing Loading, Int J. of Impact Engineering. 140 (2020) pp. 103539.

[12] G. Zhou, Q. Sun, Experiment and Simulation Study on Unidirectional Carbon Fiber Composite Component under Dynamic Three-Point Bending Loading, Int. J. of Materials and Manufacturing. 11 (2019) pp. 499-504.

[13] P. Larour, Strain rate sensitivity of automotive sheet steels: influence of plastic strain, strain rate, temperature, microstructure, bake hardening and pre-strain. RWTH Aachen. (2010)

[14] T. Emde, Mechanical behavior of metallic materials over wide ranges of strain, strain rate, and the temperature. RWTH Aachen. (2008)

[15] C. Kuhn, I. Walter, O. Taeger, T.A. Osswald, Experimental and Numerical Analysis of Fiber Matrix Separation during Compression Molding of Long Fiber Reinforced Thermoplastics. Journal of Composites Science. 1(1):2 (2017) pp. 1-16.